

**Hot-electron noise properties of graphene-like systems**

A. Rustagi and C. J. Stanton\*

*Department of Physics, University of Florida, Gainesville, Florida 32611, USA*

(Received 31 October 2013; revised manuscript received 20 October 2014; published 17 December 2014)

We study the hot-electron noise properties of two-dimensional materials with a graphene-like energy dispersion under a strong applied electric field which drives the system far from equilibrium. Calculations are based on a Boltzmann–Green-function method within a two-relaxation-time approximation that allows for both *inelastic* scattering coming from electron-phonon scattering and *elastic* scattering coming from electron-impurity scattering. The steady-state distribution function is used to calculate the average current and the low-frequency spectral density for current fluctuations (noise) in the nonequilibrium steady-state. We find that as the electric field strength *increases*, the noise *decreases* from its equilibrium thermal noise value. This is in contrast with semiconductors with a quadratic energy–wave-vector dispersion where the noise *increases* in a constant-relaxation-time model with the square of the electric field due to the Joule heating of the electron gas by the electric field. We have also studied these properties for an electronic dispersion with a gap introduced into the Dirac spectrum. The inclusion of the gap in the electronic dispersion causes an initial increase in the noise as a function of external electric field due to the heating of the electron gas for large gap values. At high electric fields, the noise decreases with increasing electric field as in the case of gapless dispersion at higher fields.

DOI: [10.1103/PhysRevB.90.245424](https://doi.org/10.1103/PhysRevB.90.245424)

PACS number(s): 72.20.Ht, 72.70.+m, 05.40.Ca

**I. INTRODUCTION**

Graphene is a promising candidate for engineering nanoscale devices because of its novel electronic properties [1,2]. The band structure of graphene is linear and gapless near the Dirac  $K$  and  $K'$  points and this leads to unusual transport properties when large external electric and magnetic fields are applied [3–9]. Graphene has been used to fabricate nanoscale devices like  $p$ - $n$  junctions [10] and field effect transistors [11,12]. There have also been attempts to introduce a small gap in its otherwise gapless dispersion by using a hexagonal boron nitride substrate [13] or by using a hydrogenated sheet of graphene [14] for device applications. These devices operate at high electric fields and room temperature.

Current fluctuations or noise are present in all electrical devices with various origins. For instance, noise due to equilibrium thermal fluctuations is called Johnson-Nyquist noise, while noise due to the discreteness of electrical charge is referred to as shot noise. Johnson-Nyquist noise is white (frequency independent) for a wide range of frequencies below the inverse carrier scattering time and can be attributed to velocity/number fluctuations of carriers (electrons and holes). In equilibrium, the Johnson-Nyquist noise is related to the low-field mobility via the fluctuation-dissipation theorem (also known as the Kubo formula or Einstein relationship between mobility and diffusion). Because of this, equilibrium noise measurements do not provide any additional information about the system that is not already included in the low-field mobility measurements. Out of equilibrium, however, the noise can change and provide additional information about the system. Two types of noise that are present out of equilibrium are  $1/f$  noise [15] and *hot-electron noise* [16]. The ubiquitous  $1/f$  noise has a spectral density  $S^I(f) \sim \bar{I}^2/f$  where  $\bar{I}$  is the average current flowing through the sample. [Note that  $1/f$  noise need not be a true nonequilibrium phenomenon and that in some systems it can be seen in equilibrium ( $\bar{I} = 0$ )

in higher-order, four-point correlation functions [17–19]]. Hot-electron noise, on the other hand, is truly a nonequilibrium phenomenon. It has a white (frequency-independent) power spectrum for frequencies below the inverse scattering time. Since most electrical measurements are done at low frequency, the hot-electron noise spectrum is essentially a low-frequency measurement. In a typical hot-electron noise experiment, one will measure the dependence of the flat, low-frequency white part of the noise spectrum (above the  $1/f$  noise) as a function of applied external field and determine how it varies from its equilibrium, Johnson-Nyquist value. Hot-electron effects and current-induced heating of carriers and their energy relaxation in graphene has been studied recently [20]. Calculations and experimental measurements for the shot noise in graphene indicate sub-Poissonian behavior with a Fano factor of  $\sim 1/3$  at the charge neutrality point and a slight reduction in doped samples [21–23].

In this paper, we focus on the hot-electron noise in macroscopic graphene samples. We show that graphene and graphene-like systems not only have novel electronic properties, but they also have unusual noise properties. The hot-electron noise decreases strongly with increasing electric field. This results from the unusual linear energy–wave-vector dispersion in graphene, which means that fluctuations in the  $\vec{k}$  states in graphene do not lead to fluctuations in the magnitude of the velocity  $|\partial\varepsilon/\partial\vec{k}|$ . Thus not only can one make unusual nanoscale devices from graphene, but we find that these devices should have excellent noise properties. Section II of this paper describes our formalism for calculating the hot-electron noise spectrum in graphene. Results are presented in Sec. III and our conclusions are given in Sec. IV.

**II. CALCULATION OF NOISE SPECTRAL DENSITY USING THE BOLTZMANN-GREEN-FUNCTION METHOD**

The Wiener-Khinchine theorem relates the noise spectral density to the Fourier transform of the current-current correlation function. The current-current correlation function for

\*Corresponding author: [avinash@phys.ufl.edu](mailto:avinash@phys.ufl.edu)

stationary processes is given by

$$\Gamma_{ij}^I(t) = \langle \delta I_i(t) \delta I_j(0) \rangle, \quad (1)$$

where  $i, j$  correspond to the spatial coordinates:  $i, j = (x, y)$ .

For uncorrelated carriers (i.e., neglecting carrier-carrier interactions), the current-fluctuation correlation function is proportional to the velocity-velocity correlation function for a single particle, which is given by

$$\Gamma_{ij}^v(t) = \langle \delta v_i(t) \delta v_j(0) \rangle. \quad (2)$$

Even in a single-particle picture, fluctuations in the carrier velocity can occur due to scattering with impurities and phonons. Since transport at high temperatures is usually calculated based on the Boltzmann transport equation, we will use a method to calculate the velocity fluctuations based on finding the Green function for the time-dependent Boltzmann equation [24].

Van Vliet *et al.* have shown that for the diffusion equation, this type of Green function approach is equivalent to adding Langevin noise terms to the diffusion equation [25]. In an analogous manner, the Boltzmann–Green-function approach to calculating the velocity fluctuations is equivalent to the Boltzmann–Langevin approach to calculating the fluctuations [26,27].

This Boltzmann–Green-function approach to the calculation of hot-electron noise has been applied to a variety of systems. These include crossover from thermal-like noise to shot noise in small-length wires [28]; hot-electron intervalley noise in multivalley semiconductors such as GaAs [29]; quantum-confined field effect transistors [30]; metallic systems [31,32]; and one-dimensional ballistic wires [33].

To get a feeling of how the noise varies with electric field in a system with a standard parabolic  $\epsilon$  vs  $k$  energy dispersion, we make a simple approximation. The low-frequency  $\omega \approx 0$  noise can be thought of as the area under the autocorrelation function. In the simplest picture, the height of the autocorrelation function is proportional to  $\langle (v - \bar{v})^2 \rangle$  while the width is proportional to  $\tau$ , the momentum relaxation time. Hence the noise should scale with external field as  $\langle v^2 \tau \rangle$ , i.e., the nonequilibrium diffusion effects. Heating of the electron gas in a parabolic system leads to  $\langle v^2 \rangle$  varying as  $E^2$ . Scattering times, however, can decrease with increasing electric field. The interplay between these effects can cause the noise to increase or decrease with electric field. If the scattering time is approximately constant, then the dominant effect is the heating of the electron gas by the external electric field, which causes an increase in the low-frequency hot-electron noise with  $E^2$ . This is in fact observed in GaAs (for small enough electric fields so that intervalley transfer into the satellite  $L$  valley does not occur). Experimental measurements observed an initial quadratic electric field dependence [34,35].

The average in the autocorrelation function in Eq. (2) is taken with respect to a joint probability distribution that the charge carrier has momentum  $\vec{k}$  at time  $t$  and momentum  $\vec{k}_0$  at time  $t = 0$  and is denoted by  $P(\vec{k}, t | \vec{k}_0, t = 0)$ . This joint probability distribution can be rewritten as the product of the conditional probability distribution  $R(\vec{k}, t | \vec{k}_0)$  and the steady-state distribution function  $f(\vec{k}_0)$ . The velocity autocorrelation

function can be simplified further [36,37]:

$$\begin{aligned} \Gamma_{ij}^v(t) &= \iiint [\delta v_i(\vec{k})][\delta v_j(\vec{k}_0)] R(\vec{k}, t | \vec{k}_0) f(\vec{k}_0) d\vec{k}_0 d\vec{k} \\ &= \iiint v_i(\vec{k}) [v_j(\vec{k}_0) - \langle v_j \rangle] R(\vec{k}, t | \vec{k}_0) f(\vec{k}_0) d\vec{k}_0 d\vec{k} \\ &= \iiint v_i(\vec{k}) v_j(\vec{k}_0) R(\vec{k}, t | \vec{k}_0) f(\vec{k}_0) d\vec{k}_0 d\vec{k} - \langle v \rangle^2 \\ &= \iint v_i(\vec{k}) g_j(\vec{k}, t) d\vec{k}, \end{aligned} \quad (3)$$

where

$$\begin{aligned} g_j(\vec{k}, t) &= \iint v_j(\vec{k}_0) [R(\vec{k}, t | \vec{k}_0) - f(\vec{k})] f(\vec{k}_0) d\vec{k}_0 \\ \langle v_j \rangle &= \iint v_j(\vec{k}) f(\vec{k}) d\vec{k} \end{aligned}$$

and the velocity, as a function of wave-vector  $\vec{k}$  can be determined from the electronic band structure  $v_i(\vec{k}) = \frac{1}{\hbar} \frac{\partial \epsilon(\vec{k})}{\partial k_i}$ . Therefore to calculate the velocity autocorrelation function, we need to evaluate  $g_j(\vec{k}, t)$ .

The noise spectral density can be evaluated by taking the time Fourier transform of the autocorrelation function. The noise spectral density is given by

$$\begin{aligned} S_{ij}(\omega) &= \frac{4Ne^2}{L^2} \text{Re} \left[ \int_0^\infty e^{-i\omega t} \Gamma_{ij}^v(t) dt \right] \\ &= \frac{4Ne^2}{L^2} \text{Re} \left[ \iint v_i(\vec{k}) g_j(\vec{k}, \omega) d\vec{k} \right], \end{aligned} \quad (4)$$

where

$$g_j(\vec{k}, \omega) = \int_0^\infty e^{-i\omega t} g_j(\vec{k}, t) dt,$$

$N$  is the total number of charge carriers,  $e$  is the charge of the carrier, and  $L$  is the length of the sample.

The Boltzmann–Green-function method is a three-step process to determine the velocity autocorrelation function. For a uniform system (no spatial dependence) these steps are as follows:

(1) Determine the steady-state solution to the Boltzmann equation  $f(\vec{k})$ .

(2) Determine the response function  $R(\vec{k}, t | \vec{k}_0, t_0)$  [or the effective distribution  $g(\vec{k}, t)$  with the initial condition  $g(\vec{k}, t = 0) = [v(\vec{k}) - \langle v \rangle] f(\vec{k})$ ] which is the solution to the full time-dependent Boltzmann equation with the initial condition  $R(\vec{k}, t = t_0 | \vec{k}_0, t_0) = \delta(\vec{k} - \vec{k}_0)$ . In the single-particle picture, this is the conditional probability for finding a particle at time  $t$  with momentum  $\vec{k}$  given that it started out with momentum  $\vec{k}_0$  at time  $t_0$ .

(3) Calculate the velocity autocorrelation function  $\Gamma^v(t)$  from the effective distribution function  $g(\vec{k}, t)$ . Taking the Fourier cosine transform with respect to time yields the power spectrum. Since most electrical noise measurements are made at frequencies much lower than the inverse carrier scattering times, we effectively measure the  $\omega \rightarrow 0$  limit of the power spectrum as a function of the applied external field  $S^I(\omega = 0, E)$ . Again, it is understood that this corresponds to the flat, white-noise portion of the power spectrum above any

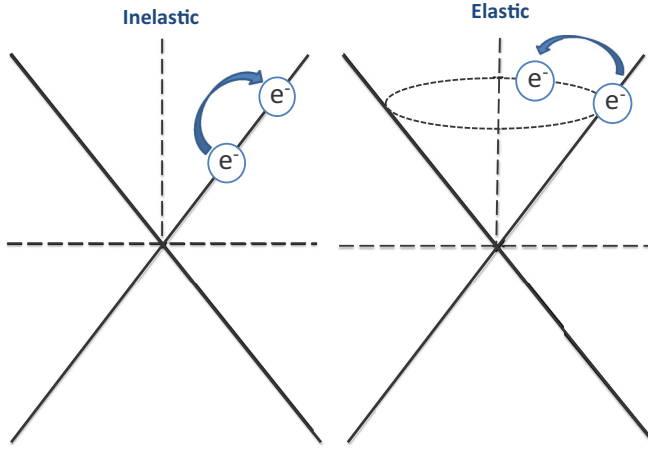


FIG. 1. (Color online) The diagram shows the effect of the two distinct scattering mechanisms. Inelastic scattering allows for change in energy by scattering between states of different energy while elastic scattering corresponds to scattering between different momentum states with the same energy.

$1/f$  noise contribution.  $1/f$  noise is a different type of noise and is not the focus of this paper.

The calculation of the spectral density requires the steady-state distribution function  $f(\vec{k}_0)$ . For our model, the steady-state distribution function is evaluated by solving the Boltzmann equation within the relaxation-time approximation. We include two different relaxation times in our model. The collision integral has two terms that include the effects of two distinct types of scattering mechanisms [38]. The first term corresponds to inelastic scattering where the collisions try to drive the steady-state distribution function back to the equilibrium distribution function  $f_{\text{eq}}(\vec{k})$ . This type of scattering represents electron-phonon scattering since phonons take energy (and also momentum) out of the electron system. We note that the equilibrium distribution is a Fermi-Dirac distribution

$$f_{\text{eq}}(\vec{k}) = [1 + e^{\beta(\epsilon(\vec{k}) - \mu)}]^{-1} \quad \text{where} \quad \beta = \frac{1}{k_B T}. \quad (5)$$

The second term corresponds to elastic scattering where the collisions try to drive the steady-state distribution to its angular average by changing the momentum on scattering but not the energy (see Fig. 1). Elastic scattering is typically electron-impurity scattering. Elastic scattering cannot take energy out of the electron system, but can take momentum out of the system.

The collision integral is given by [39]

$$I_{\text{collision}} = -\frac{f(\vec{k}) - f_{\text{eq}}(\vec{k})}{\tau_{\text{in}}} - \frac{f(\vec{k}) - \langle f(\vec{k}) \rangle_{\theta}}{\tau_{\text{el}}}, \quad (6)$$

where  $f(\vec{k})$  is the steady-state distribution function,  $f_{\text{eq}}(\vec{k})$  is the equilibrium distribution function,  $\langle f(\vec{k}) \rangle_{\theta}$  is the angular average of the steady-state distribution function,  $\tau_{\text{in}}$  is the inelastic scattering time, and  $\tau_{\text{el}}$  is the elastic scattering time. We note that we have omitted electron-electron scattering from our model. Electron-electron scattering typically thermalizes the distribution to one with an effective electron temperature

(i.e., the hot-electron temperature) which is greater than that of the lattice. In electron-electron scattering, the total energy of both electrons is conserved in the scattering process as well as the sum of the wave vectors (neglecting umklapp processes). Thus, in a system with a parabolic energy-wave-vector dispersion, electron-electron scattering cannot degrade the total current (momentum) and does not contribute substantially to the noise. However, in systems like graphene where the energy-wave-vector dispersion is linear, momentum and wave vector are different and as a result, electron-electron scattering can take momentum out of the system. We note that a recent Monte Carlo study indicates that in monolayer graphene there is very little effect due to electron-electron scattering on transport properties at high carrier densities, but that there can be an effect for small carrier densities [40]. They find that the inclusion of electron-electron collisions leads to a reduction of the total overall current at low densities (but not at high densities). In our model, we consider the generic effects of any scattering mechanism that can lead to energy change (inelastic scattering) as well as those mechanisms which conserve energy but change the momentum (direction) of the carriers.

Assuming spatial homogeneity and under the application of an external electric field  $\vec{E} = -E\hat{x}$  in the  $x$  direction, the Boltzmann equation for the steady-state distribution function is given by

$$\frac{eE}{\hbar} \frac{\partial f(\vec{k})}{\partial k_x} = -\frac{f(\vec{k}) - f_{\text{eq}}(\vec{k})}{\tau_{\text{in}}} - \frac{f(\vec{k}) - \langle f(\vec{k}) \rangle_{\theta}}{\tau_{\text{el}}}, \quad (7)$$

where the electron charge is  $-e$  (the force  $\vec{F} = -e\vec{E} = eE\hat{x}$ ). To solve the above equation, we use the two-dimensional (2D) Fourier transform defined by

$$F(\vec{r}) = \frac{1}{2\pi} \iint e^{-i\vec{k}\cdot\vec{r}} f(\vec{k}) d\vec{k}, \quad (8)$$

$$f(\vec{k}) = \frac{1}{2\pi} \iint e^{i\vec{k}\cdot\vec{r}} F(\vec{r}) d\vec{r}.$$

Here  $\vec{r} = (x, y)$  is the Fourier-space conjugate to the momentum. In Fourier space the Eq. (7) can be rewritten as

$$\frac{ieEx}{\hbar} F(\vec{r}) = -\frac{F(\vec{r}) - F_{\text{eq}}(\vec{r})}{\tau_{\text{in}}} - \frac{F(\vec{r}) - \langle F(\vec{r}) \rangle_{\theta}}{\tau_{\text{el}}}. \quad (9)$$

Defining  $\tau^{-1} = \tau_{\text{in}}^{-1} + \tau_{\text{el}}^{-1}$  and  $p_D = eE\tau/\hbar$ , the equation becomes

$$F(\vec{r}) = \frac{1}{(1 + ip_D x)} \left[ \frac{\tau}{\tau_{\text{in}}} F_{\text{eq}}(\vec{r}) + \frac{\tau}{\tau_{\text{el}}} \langle F(\vec{r}) \rangle_{\theta} \right]. \quad (10)$$

Taking the angular average of both sides and solving for  $\langle F(\vec{r}) \rangle_{\theta}$ , we get

$$\langle F(\vec{r}) \rangle_{\theta} = \frac{\tau}{\tau_{\text{in}}} \frac{F_{\text{eq}}(\vec{r})}{\sqrt{1 + p_D^2 r^2 - \frac{\tau}{\tau_{\text{el}}}}}. \quad (11)$$

Substituting the angular average back in Eq. (10), we get

$$F(\vec{r}) = \frac{\tau F_{\text{eq}}(\vec{r}) \sqrt{1 + p_D^2 r^2}}{\tau_{\text{in}} (1 + ip_D x) \left[ \sqrt{1 + p_D^2 r^2 - \frac{\tau}{\tau_{\text{el}}}} \right]}. \quad (12)$$

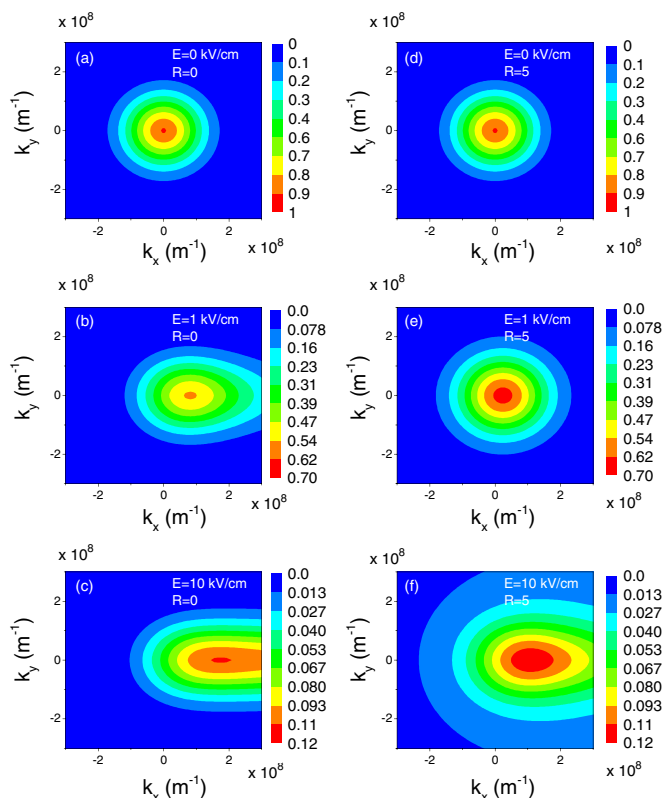


FIG. 2. (Color online) Comparison between contour plots for the steady-state distribution function  $f(\vec{k})$  on varying the scattering-rate ratio  $R$  and field  $E$  for a fixed electron density  $n = 10^{11} \text{ cm}^{-2}$  at  $T = 300 \text{ K}$ . (a)  $E = 0 \text{ kV/cm}$ ,  $R = 0$ , (b)  $E = 1 \text{ kV/cm}$ ,  $R = 0$ , (c)  $E = 10 \text{ kV/cm}$ ,  $R = 0$ , (d)  $E = 0 \text{ kV/cm}$ ,  $R = 5$ , (e)  $E = 1 \text{ kV/cm}$ ,  $R = 5$ , and (f)  $E = 10 \text{ kV/cm}$ ,  $R = 5$ , for Dirac-like dispersion. The plots indicate that the presence of a strong elastic scattering mechanism takes momentum from the field direction and transfers it over the constant-energy surface. Note: The color-bar scales are different for different fields.

Thus given any equilibrium distribution, we can determine the steady-state distribution in the presence of an electric field,

$$f(\vec{k}) = \frac{1}{(2\pi)\tau_{\text{in}}} \iint d\vec{r} \frac{e^{i\vec{k}\cdot\vec{r}} \tau F_{\text{eq}}(\vec{r})}{(1 + i p_D x)} \left[ \frac{\sqrt{1 + p_D^2 r^2}}{\sqrt{1 + p_D^2 r^2 - \frac{\tau}{\tau_{\text{el}}}}} \right].$$

We define the variable  $R = \tau_{\text{in}}/\tau_{\text{el}}$  as the ratio of the elastic to the inelastic scattering rate. Using the equilibrium distribution function of the form in Eq. (5) for Dirac-like dispersion, the steady-state distribution is evaluated for various combinations of the ratio of the elastic scattering rate to the inelastic scattering rate  $R$  and electric field  $E$  (see Fig. 2). The effect of the electric field is to force the carriers to drift strongly along the field direction as seen in Figs. 2(a)–2(c). However, upon the introduction of the elastic scattering mechanism, the elastic scattering tries to make the distribution symmetric in the  $k_x$ - $k_y$  plane and hence the spread of the distribution in the field direction is reduced [see Figs. 2(d)–2(f)]. To get a better understanding of these features, one can look at the steady-state distribution function plotted as a function of  $k_x$  for a fixed  $k_y = 0$  for different field strengths and scattering

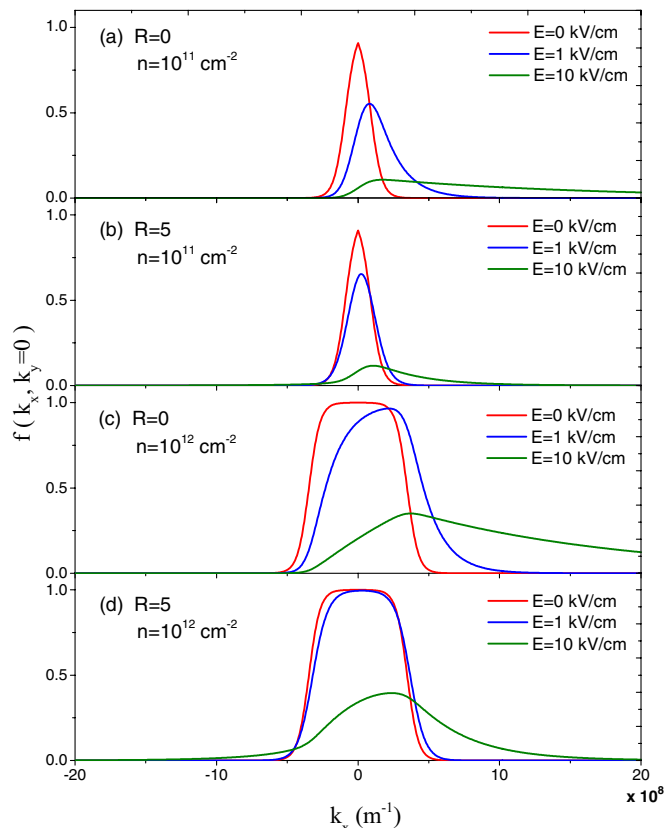


FIG. 3. (Color online) Steady-state distribution vs  $k_x$  at fixed  $k_y = 0$  for different electric field strengths at  $T = 300 \text{ K}$ . For number density  $n = 10^{11} \text{ cm}^{-2}$ . (a) Scattering ratio  $R = 0$ , meaning the presence of only inelastic scattering; (b) scattering ratio  $R = 5$ , meaning the presence of strong elastic scattering. For comparison purposes the case of a higher carrier density  $n = 10^{12} \text{ cm}^{-2}$  is considered. (c) and (d) show the equilibrium Fermi-Dirac distribution and the effects of scattering-rate ratio  $R$  on the steady-state distribution.

ratios (see Fig. 3). In Fig. 3(a), with no elastic scattering, it is clearly seen that the normalized distribution function drifts in the direction of the electric field with increasing field strength. However, on inclusion of the elastic scattering term, the elastic scattering reduces the effect of the field as seen in Fig. 3(b). Note that Fig. 3 clearly shows that the equilibrium distribution is not Gaussian.

Similarly, the calculation for the steady-state distribution can be made for a gapped Dirac spectrum  $\epsilon(\vec{k}) = \sqrt{\Delta^2/4 + (\hbar v_f k)^2}$  [see Figs. 4(a)–4(f)] and similar effects of the field and scattering ratio are seen. We note that the typical energies where deviations from linear Dirac dispersion come about is  $\sim 2 \text{ eV}$ , which corresponds to a wave-vector magnitude of about  $30 \times 10^8 \text{ m}^{-1}$ . As seen from Fig. 3, even for high field strengths of  $\sim 10 \text{ kV/cm}$  the distribution is still mainly restricted to lower energies and thus we do not consider the full dispersion for our calculations.

The next step in determining the noise spectrum is to solve for the conditional probability  $R(\vec{k}, t | \vec{k}_0)$  defined as the probability to find a carrier with momentum  $\vec{k}$  at time  $t$  given that it had momentum  $\vec{k}_0$  at time  $t = 0$ . Thus the initial condition for the conditional probability is

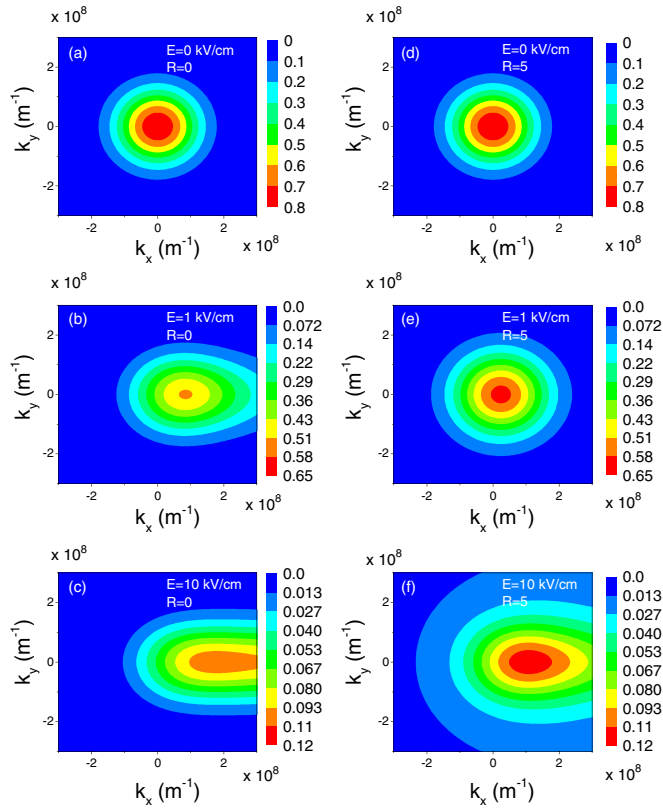


FIG. 4. (Color online) Comparison between contour plots for the steady-state distribution function  $f(\vec{k})$  on varying the scattering-rate ratio  $R$  and field  $E$  for a fixed electron density  $n = 10^{11} \text{ cm}^{-2}$  at  $T = 300 \text{ K}$ . (a)  $E = 0 \text{ kV/cm}$ ,  $R = 0$ , (b)  $E = 1 \text{ kV/cm}$ ,  $R = 0$ , (c)  $E = 10 \text{ kV/cm}$ ,  $R = 0$ , (d)  $E = 0 \text{ kV/cm}$ ,  $R = 5$ , (e)  $E = 1 \text{ kV/cm}$ ,  $R = 5$ , and (f)  $E = 10 \text{ kV/cm}$ ,  $R = 5$ , for gapped Dirac-like dispersion ( $\Delta = 60 \text{ meV}$ ). The plots indicate that the presence of a strong elastic scattering mechanism takes momentum from the field direction and transfers it over the constant-energy surface. Note: The color-bar scales are different for different fields.

$R(\vec{k}, t = 0 | \vec{k}_0) = \delta(\vec{k} - \vec{k}_0)$ . The motion of the carrier within the semiclassical framework is still governed by the Boltzmann equation. Thus one can write an equation obeyed by the conditional probability in the presence of an electric field and the two scattering mechanisms.

$$\frac{dR}{dt} = \frac{\partial R}{\partial t} + \frac{eE}{\hbar} \frac{\partial R}{\partial k_x} = -\frac{R - f_{\text{eq}}}{\tau_{\text{in}}} - \frac{R - \langle R \rangle_{\theta}}{\tau_{\text{el}}}. \quad (13)$$

Defining

$$\xi(\vec{k}, t; \vec{k}_0) = R(\vec{k}, t | \vec{k}_0) - f(\vec{k}),$$

and subtracting Eq. (7) from Eq. (13), we get

$$\frac{\partial \xi}{\partial t} + \frac{eE}{\hbar} \frac{\partial \xi}{\partial k_x} = -\frac{\xi}{\tau_{\text{in}}} - \frac{\xi - \langle \xi \rangle_{\theta}}{\tau_{\text{el}}}. \quad (14)$$

Multiplying the above equation by  $v_j(\vec{k}_0) f(\vec{k}_0)$  and integrating over  $\vec{k}_0$ :

$$\frac{\partial g_j(\vec{k}, t)}{\partial t} + \frac{eE}{\hbar} \frac{\partial g_j(\vec{k}, t)}{\partial k_x} = -\frac{g_j(\vec{k}, t)}{\tau_{\text{in}}} - \frac{g_j(\vec{k}, t) - \langle g_j(\vec{k}, t) \rangle_{\theta}}{\tau_{\text{el}}}, \quad (15)$$

where  $g$  is defined in Eq. (3) and satisfies the initial condition

$$g_j(\vec{k}, t = 0) = [v_j(\vec{k}) - \langle v_j \rangle] f(\vec{k}). \quad (16)$$

Taking the Fourier transform in time of Eq. (15),

$$\begin{aligned} i\omega g_j(\vec{k}, \omega) + \frac{eE}{\hbar} \frac{\partial g_j(\vec{k}, \omega)}{\partial k_x} \\ = [v_j(\vec{k}) - \langle v_j \rangle] f(\vec{k}) - \frac{g_j(\vec{k}, \omega)}{\tau_{\text{in}}} - \frac{g_j(\vec{k}, \omega) - \langle g_j(\vec{k}, \omega) \rangle_{\theta}}{\tau_{\text{el}}}. \end{aligned} \quad (17)$$

To solve the above equation, we again use the 2D Fourier transforms,

$$\begin{aligned} G_j(\vec{r}, \omega) &= \frac{1}{2\pi} \iint e^{-i\vec{k}\cdot\vec{r}} g_j(\vec{k}, \omega) d\vec{k}, \\ g_j(\vec{k}, \omega) &= \frac{1}{2\pi} \iint e^{i\vec{k}\cdot\vec{r}} G_j(\vec{r}, \omega) d\vec{r}. \end{aligned} \quad (18)$$

Equation (17) in Fourier space becomes

$$\begin{aligned} i\omega G_j(\vec{r}, \omega) + \frac{ieEx}{\hbar} G_j(\vec{r}, \omega) \\ = h_j(\vec{r}) - \frac{G_j(\vec{r}, \omega)}{\tau_{\text{in}}} - \frac{G_j(\vec{r}, \omega) - \langle G_j(\vec{r}, \omega) \rangle_{\theta}}{\tau_{\text{el}}}, \end{aligned} \quad (19)$$

where  $h_j(\vec{r}) = \frac{1}{2\pi} \iint e^{-i\vec{k}\cdot\vec{r}} [v_j(\vec{k}) - \langle v_j \rangle] f(\vec{k}) d\vec{k}$ .

To study the low-frequency noise, we set  $\omega = 0$ , and then Eq. (19) is solved for  $G_j(\vec{r}, \omega = 0)$ :

$$G_j(\vec{r}, \omega = 0) = \frac{1}{(1 + ip_{Dx})} \left[ \tau h_j(\vec{r}) + \frac{\tau}{\tau_{\text{el}}} \langle G_j(\vec{r}, \omega = 0) \rangle_{\theta} \right]. \quad (20)$$

Taking the angular average on both sides, we get

$$\langle G_j(\vec{r}, \omega = 0) \rangle_{\theta} = \frac{\tau \sqrt{1 + p_D^2 r^2}}{\sqrt{1 + p_D^2 r^2 - \frac{\tau}{\tau_{\text{el}}}}} \left\langle \frac{h_j(\vec{r})}{1 + ip_{Dx}} \right\rangle_{\theta}. \quad (21)$$

Thus the final expression for  $G_j(\vec{r}, \omega = 0)$  is

$$\begin{aligned} G_j(\vec{r}, \omega = 0) \\ = \frac{\tau h_j(\vec{r})}{1 + ip_{Dx}} + \frac{(\tau^2/\tau_{\text{el}}) \sqrt{1 + p_D^2 r^2}}{\sqrt{1 + p_D^2 r^2 - \frac{\tau}{\tau_{\text{el}}}}} \left\langle \frac{h_j(\vec{r})}{1 + ip_{Dx}} \right\rangle_{\theta}. \end{aligned}$$

The function  $g_j(\vec{k}, \omega = 0)$  can be obtained by taking the inverse Fourier transform of the above function  $G_j(\vec{r}, \omega = 0)$ :

$$\begin{aligned} g_j(\vec{k}, \omega = 0) &= g_j^I + g_j^{II}, \\ g_j^I &= \frac{1}{2\pi} \iint e^{i\vec{k}\cdot\vec{r}} \frac{\tau h_j(\vec{r})}{1 + ip_{Dx}} d\vec{r}, \\ g_j^{II} &= \int r \frac{(\tau^2/\tau_{\text{el}}) J_0(kr)}{1 - \frac{(\tau/\tau_{\text{el}})}{\sqrt{1 + p_D^2 r^2}}} \left\langle \frac{h_j(\vec{r})}{1 + ip_{Dx}} \right\rangle_{\theta} dr, \end{aligned}$$

where the integrand in  $g_j^{II}$  has the zeroth-order Bessel function  $J_0$  which is a function of the magnitude of the wave-vector  $k$

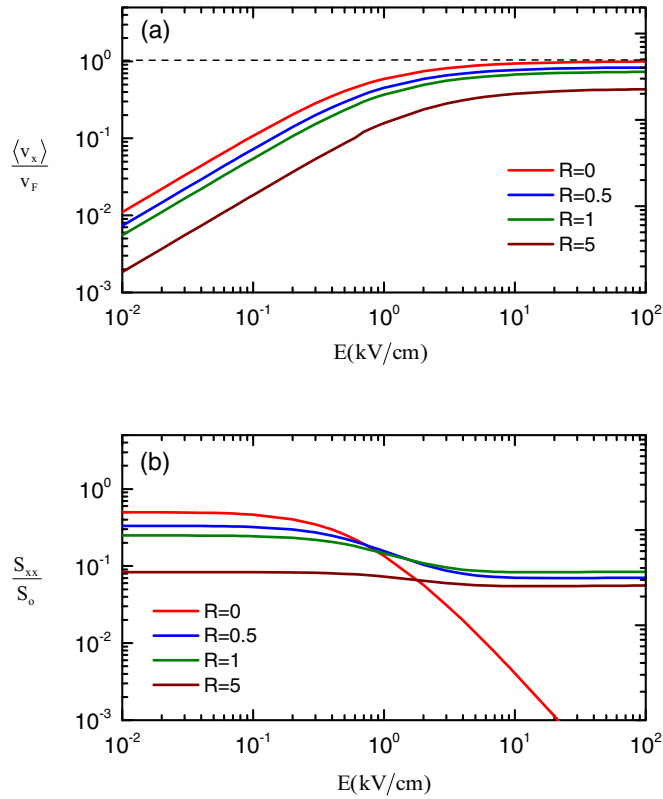


FIG. 5. (Color online) (a) Average  $x$  component of velocity, and (b) zero-frequency noise versus electric field for a Dirac-like dispersion  $\epsilon(\vec{k}) = \hbar v_f k$  on varying the value of  $R$  (the ratio of elastic scattering rate to inelastic scattering rate) where  $n = 10^{11} \text{ cm}^{-2}$  and  $T = 300 \text{ K}$ . The plots for the case of a higher carrier density  $n = 10^{12} \text{ cm}^{-2}$  look extremely similar. Note:  $S_o = 4Ne^2 v_f^2 \tau_{in} / L^2$ .

and the magnitude of the Fourier-space coordinate  $r$ . Thus the low-frequency noise is

$$S_{ij}(\omega = 0) = \frac{4Ne^2}{L^2} \text{Re} \left[ \iint v_i(\vec{k}) [g_j^I + g_j^{II}] d\vec{k} \right]. \quad (22)$$

Now since  $v_i(\vec{k})$  is odd in the variable  $k_i$  (if  $E$  is applied in the  $i$ th direction) and  $g_j^{II}$  is even in  $k_i$ , the integral of  $v_i(\vec{k})g_j^{II}(\vec{k})$  over all  $\vec{k}$  is zero. Thus for evaluating the low-frequency noise, we simply need to evaluate the first term, which is given by

$$S_{ij}(\omega = 0) = \frac{4Ne^2}{L^2} \text{Re} \left[ \iint v_i(\vec{k}) g_j^I(\vec{k}, \omega = 0) d\vec{k} \right], \quad (23)$$

where

$$g_j^I(\vec{k}, \omega = 0) = \frac{1}{2\pi} \iint e^{i\vec{k}\cdot\vec{r}} \frac{\tau h_j(\vec{r})}{1 + ip_D x} d\vec{r}.$$

We note that because we have used a relaxation-time approximation, we have an analytical solution to the problem (in terms of integrals which are evaluated numerically).

### III. RESULTS AND DISCUSSION

The results of the noise calculation for a Dirac-like dispersion  $\epsilon(\vec{k}) = \hbar v_f k$  ( $v_f$  is the Fermi velocity) are calculated and shown in Fig. 5 for  $n = 10^{11} \text{ cm}^{-2}$  at room temperature.

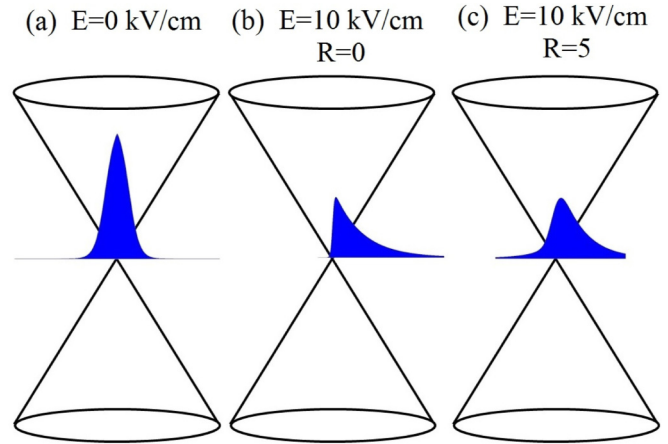


FIG. 6. (Color online) Toy diagram to show the occupancy of states in the Dirac cone under the effect of electric field and scattering-rate ratio. (a)  $E = 0 \text{ kV/cm}$  where the distribution is the equilibrium distribution function. (b)  $E = 10 \text{ kV/cm}$  and  $R = 0$ , meaning a moderate field and just inelastic scattering, and the distribution drifts in the direction of the field, occupying large- $k_x$  states. (c)  $E = 10 \text{ kV/cm}$  and  $R = 5$ , meaning a moderate field and the presence of large elastic scattering along with inelastic scattering, such that the distribution drifts in the direction of the field; however, the elastic scattering reduces the spread in the field direction.

The average of the  $x$  component of velocity is evaluated as a function of electric field for various ratios of the elastic to inelastic scattering rates [see Fig. 5(a)]. As the field increases, the distribution drifts in the direction of the field (see Fig. 6) occupying states with large  $v_x$  and thus the average velocity increases, reaching the saturation value  $v_f$  for high field strengths.

However, the increase of the ratio of scattering rates reduces the spread of the steady-state distribution function in the field direction by scattering on to the constant-energy states (see Fig. 6); thus it takes even higher fields to reach the saturation value. The low-frequency spectral density is also plotted as a function of field strength for varying scattering-rate ratio  $R$  [see Fig. 5(b)]. At low field strengths, the noise is constant as a function of  $E$  in agreement with the Johnson-Nyquist noise value. Increase in  $R$  reduces the low-field noise. Low field values correspond to the linear response regime where the noise spectrum is proportional to the conductivity  $\sigma$  (or inversely proportional to the resistance  $R$ ) given by the current-current correlation

$$S^I = \frac{4k_B T}{R} \sim 4k_B T \sigma. \quad (24)$$

The conductivity is proportional to the mobility, which is proportional to the inverse scattering rate  $\tau = \tau_{in} / (1 + R)$ . Thus the increase in  $R$  implies the presence of elastic scattering reduces the low-field mobility as obtained by the Monte Carlo simulation results [4]. However, at high field strengths, the noise for  $R = 0$ , i.e., with only inelastic scattering, decreases, but for finite  $R$ , i.e., the presence of both scattering mechanisms, the noise decreases at a slower rate. At large fields the distribution function drifts considerably in the direction of the field, and inelastic scattering of carriers brings about

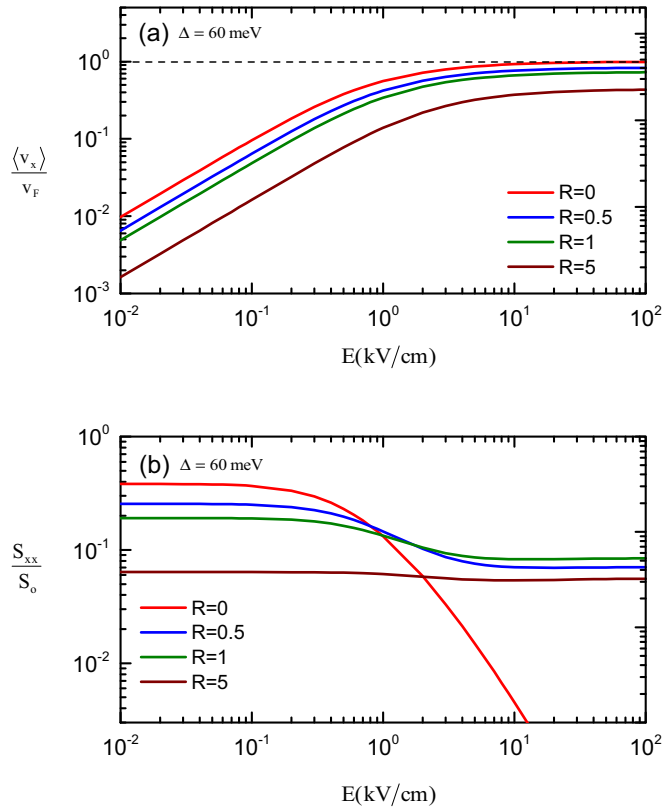


FIG. 7. (Color online) (a) Average  $x$  component of velocity, and (b) zero-frequency noise versus electric field for a gapped Dirac-like dispersion  $\epsilon(\vec{k}) = \sqrt{\Delta^2/4 + (\hbar v_f k)^2}$  on varying the value of  $R$  (the ratio of the elastic scattering rate to the inelastic scattering rate) where  $n = 10^{11} \text{ cm}^{-2}$  and  $T = 300 \text{ K}$ . The value of the gap is  $\Delta = 60 \text{ meV}$ . Note:  $S_o = 4Ne^2v_f^2\tau_{in}/L^2$ .

change in the  $\vec{k}$  states, but the velocity which is given by the gradient of the energy dispersion does not change in magnitude; it only slightly changes in direction since scattering is predominantly in the field direction. Thus we see that for only inelastic scattering, the noise decreases and continues to decrease with increasing electric field. When we include an elastic scattering mechanism (such as impurity scattering), we see that the noise also decreases but not as much or as rapidly as a function of electric field. This is in contrast to regular semiconductors with a parabolic energy dispersion ( $\epsilon \propto k^2$ ), where in a constant-relaxation-time model with elastic and inelastic scattering the noise increases with electric field as  $E^2$  due to Joule heating of the electron gas. Thus, under high-field conditions, devices based on graphene will have *better noise properties* than conventional semiconductors with quadratic energy-wave-vector dispersions.

It is also possible to introduce a gap parameter in the energy dispersion to study the noise properties of “graphene-like” systems. This is equivalent to the dispersion for narrow-gap semiconductors  $\epsilon(\vec{k})(1 + \alpha\epsilon(\vec{k})) = \hbar^2 k^2 / 2m^*$ . The modified energy dispersion for graphene with gap  $\Delta$  is  $\epsilon(\vec{k}) = \sqrt{\Delta^2/4 + \hbar^2 v_f^2 k^2}$ . The results for the current and noise for  $\Delta = 60 \text{ meV}$  (see Fig. 7) and for the results for  $\Delta = 1000 \text{ meV}$  (see Fig. 8) are shown. The average of the  $x$  component of

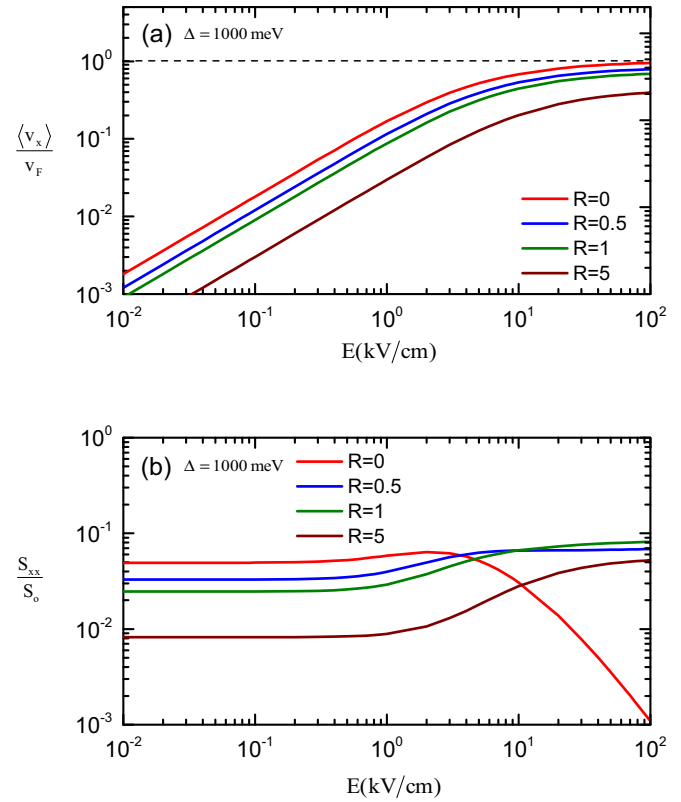


FIG. 8. (Color online) (a) Average  $x$  component of velocity, and (b) zero-frequency noise versus electric field for a gapped Dirac-like dispersion  $\epsilon(\vec{k}) = \sqrt{\Delta^2/4 + (\hbar v_f k)^2}$  on varying the value of  $R$  (the ratio of the elastic scattering rate to the inelastic scattering rate) where  $n = 10^{11} \text{ cm}^{-2}$  and  $T = 300 \text{ K}$ . The value of gap is  $\Delta = 1000 \text{ meV}$ . Note:  $S_o = 4Ne^2v_f^2\tau_{in}/L^2$ .

velocity is evaluated as a function of electric field for various values of the scattering-rate ratio [see Figs. 7(a) and 8(a)]. As the field increases, the average velocity increases, reaching the saturation value  $v_f$  for large values of the field. However, the increase of the scattering-rate ratio reduces the increase in the average velocity and the saturation value is reached at even higher values of field. The noise spectral density is evaluated for gapped graphene-like dispersion [see Figs. 7(b) and 8(b)]. The figures show that the noise is the thermal Johnson-Nyquist noise at low fields. The plots for the noise spectral density do not show a significant difference from that for a gapless dispersion case for  $\Delta = 60 \text{ meV}$ . The carrier density  $n = 10^{11} \text{ cm}^{-2}$  (chosen to avoid thermally exciting carriers from the valence to the conduction band) used for the calculations ensures that the unoccupied  $\vec{k}$  states are in the linear part of the dispersion and thus have a constant velocity magnitude such that the phase space for scattering does not bring about velocity fluctuations. The noise in the case of  $\Delta = 1000 \text{ meV}$  shows heating effects coming into effect for the cases of substantial elastic scattering. At  $\Delta = 1000 \text{ meV}$  ( $=1 \text{ eV}$ ) the gap is similar to that in conventional semiconductors and one once again gets the increase in the noise with electric field. This can be understood by the fact that at intermediate fields the carriers occupy small- $\vec{k}$  states for which the leading-order Taylor series expansion of the

energy dispersion is quadratic in  $k$ . In an earlier study done for a parabolic energy dispersion with a constant relaxation time, it was seen that noise increases with field strength due to heating of the electron gas by the electric field [24]. Thus there are heating effects for intermediate fields; however, at high field strengths the carriers drift to the large- $\vec{k}$  states and the noise follows the graphene dispersion trend. The effect of the elastic scattering term is that higher field strength is required to cause heating. It is further noted that an increase in the gap causes an increase in the heating. The heating effect is much more prominent in dispersions with large gap parameter. We note that such high values of the gap parameter are not realized in graphene but this result shows the consistency of this method. This behavior of noise can be seen in systems with small gaps at lower temperatures, where the Fermi distribution does not have a long thermal tail.

The decrease in the noise as a function of electric field is fairly easy to understand. The power spectrum at  $\omega = 0$  as a function of electric field is proportional to the area under the velocity autocorrelation function,

$$S_{ij}^I(\omega = 0, E) \propto \int_0^\infty dt \langle v_i(t)v_j(0) \rangle. \quad (25)$$

In a normal system with a parabolic energy dispersion, two effects can contribute to the noise. (1) Heating of the electron gas by the applied external electric field increases the values of the  $t = 0$  velocity autocorrelation function  $\langle v^2 \rangle$ . This is essentially the increase of the *effective temperature* of the electron distribution and causes the noise to go up with increasing electric field. (2) If the scattering rates increase as a function of carrier energy, then fluctuations can damp out more quickly. This leads to a decrease in the noise. The actual behavior of the hot-electron noise with applied external electric field is a competition between these two effects.

In a system with a nonparabolic or Dirac-like energy dispersion, an additional effect plays a role. When the electrons are heated up by the external field, they go to higher energy. The heating of the electron gas leads to an increase in temperature and more fluctuations in the  $k$  states. These fluctuations in  $k$  states, however, do not necessarily lead to fluctuations in the velocity. This is because the magnitude of the velocity  $v(k) = \partial\epsilon/\partial k$  is a constant. Hence, *fluctuations in  $k$  states do not lead to fluctuations in the magnitude of the velocity*. Only the direction of the velocity can change. At zero electric field, the carrier distribution function is centered around  $k = 0$ .  $k$ -state fluctuations can have a substantial effect on the *direction* of the velocity. At high electric fields, the carrier distribution function is pushed up to higher  $k$  states in the direction of the electric field. Fluctuations in  $k$  states now no longer lead to such strong fluctuations in the direction of the velocity. The decrease in the low-frequency noise spectral density has also been calculated using the ensemble Monte Carlo method [41]. Decrease in noise has been predicted theoretically [24] for nonparabolic dispersions and has been measured experimentally in a GaAs/GaAlAs superlattice [42]. While the models used here, such as constant relaxation times, etc., are somewhat simplified, the results should be robust and apply to more realistic systems.

Some of the improvements that could be made in the future to the model include the following:

(1) *Wave-vector-dependent relaxation times*. Usually, scattering rates increase with energy. As a result, as discussed above, the fluctuations will die out faster as the carriers are accelerated to higher energy where the scattering increases. This leads to an *additional decrease* in the hot-electron noise and should not change our conclusions that the nonparabolic energy dispersion relation in graphene-like systems leads to a decrease in the hot-electron noise with increasing electric field.

(2) *Generation-recombination noise*. We have not considered scattering between the  $K$  and  $K'$  points of the Brillouin zone which involves a zone-edge ( $K$ -point) phonon and usually requires very energetic electrons. In GaAs, this type of intervalley scattering between the  $\Gamma$  and  $L$  valleys decreases the mobility and causes the noise to decrease. But in graphene, since the valleys are identical, there should be minimal effect. The calculations we have presented assumed only a single Dirac cone (i.e., electrons only and no holes). This approximation is valid provided the Fermi energy is large compared to the temperature. At room temperature, this criterion leads to a carrier density estimate of  $n = g_s \times g_v \times 2.46 \times 10^{10} \text{ cm}^{-2}$  (where  $g_{s/v}$  refers to spin/valley degeneracy). For low-carrier-density systems, one would have to take into account scattering that could generate electron-hole pairs as well as their recombination.

One other point that we note is that graphene systems are known to have low  $1/f$  noise [11,12]. As mentioned earlier, the Voss-Clarke experiment [17] showed that  $1/f$  noise can be thought of as “time-dependent” resistance fluctuations which needs a net current flowing through the sample to be observed in the two-point current-current correlation function, but can be seen with no net current in the four-point correlation function. As we have shown, the unique dispersion relation of graphene means that fluctuations in  $k$  states do not necessarily give rise to current fluctuations. As a result, we would not only expect the hot-electron noise to be low in graphene, but we would also expect  $1/f$  noise to be low.

#### IV. CONCLUSION

We have shown that in addition to all of its remarkable transport and optical properties, graphene should have very good noise properties. In the presence of an external electric field, the hot-electron noise should drop from the equilibrium Johnson-Nyquist value. This decrease in noise is easy to understand. Due to graphene’s band structure, fluctuations in  $\vec{k}$  states do not lead to changes in the magnitude of the velocity, only its direction. At equilibrium or low electric field, scattering can lead to substantial changes in direction. In strong electric fields, the carrier distribution function can be moved far up the Dirac cone in the direction of the electric field. Changes in the direction of the velocity are not as large.

The inclusion of elastic scattering mechanisms such as carrier-impurity scattering can affect the noise in two ways:

(1) Increased impurity scattering lowers the mobility and makes it harder to push the carriers up the Dirac cone.

(2) Impurity scattering drives the distribution function not towards the equilibrium distribution, but towards its angular average. As a result, impurity scattering can lead to larger changes in the direction of velocity than inelastic scattering.

For a Dirac-dispersion with a small gap, the hot-electron noise can initially increase with electric field at intermediate field values before ultimately decreasing. This occurs in the quadratic part of the energy band where heating effects can lead to an increase in noise.

Finally, while parasitics such as contact noise might be the ultimate source of noise in graphene devices, our calculations show that graphene devices should have excellent noise properties.

#### ACKNOWLEDGMENT

This work was supported by the National Science Foundation through Grant No. OISE-0968405.

- 
- [1] K. Novoselov, A. K. Geim, S. Morozov, D. Jiang, M. K. I. Grigorieva, S. Dubonos, and A. Firsov, *Nature (London)* **438**, 197 (2005).
- [2] A. H. Castro Neto, F. Guinea, N. M. R. Peres, K. S. Novoselov, and A. K. Geim, *Rev. Mod. Phys.* **81**, 109 (2009).
- [3] V. E. Dorgan, A. Behnam, H. J. Conley, K. I. Bolotin, and E. Pop, *Nano Lett.* **13**, 4581 (2013).
- [4] J. Chauhan and J. Guo, *Appl. Phys. Lett.* **95**, 023120 (2009).
- [5] M. L. Sadowski, G. Martinez, M. Potemski, C. Berger, and W. A. de Heer, *Phys. Rev. Lett.* **97**, 266405 (2006).
- [6] Z. Jiang, E. A. Henriksen, L. C. Tung, Y.-J. Wang, M. E. Schwartz, M. Y. Han, P. Kim, and H. L. Stormer, *Phys. Rev. Lett.* **98**, 197403 (2007).
- [7] M. Orlita, C. Faugeras, P. Plochocka, P. Neugebauer, G. Martinez, D. K. Maude, A.-L. Barra, M. Sprinkle, C. Berger, W. A. de Heer *et al.*, *Phys. Rev. Lett.* **101**, 267601 (2008).
- [8] R. S. Deacon, K.-C. Chuang, R. J. Nicholas, K. S. Novoselov, and A. K. Geim, *Phys. Rev. B* **76**, 081406 (2007).
- [9] L. G. Booshehri, C. H. Mielke, D. G. Rickel, S. A. Crooker, Q. Zhang, L. Ren, E. H. H aroz, A. Rustagi, C. J. Stanton, Z. Jin *et al.*, *Phys. Rev. B* **85**, 205407 (2012).
- [10] L. M. Zhang and M. M. Fogler, *Phys. Rev. Lett.* **100**, 116804 (2008).
- [11] G. Liu, W. Stillman, S. Rumyantsev, Q. Shao, M. Shur, and A. A. Balandin, *Appl. Phys. Lett.* **95**, 033103 (2009).
- [12] Q. Shao, G. Liu, D. Teweldebrhan, A. A. Balandin, S. Runyantsev, M. S. Shur, and D. Yan, *IEEE Electron Device Lett.* **30**, 288 (2009).
- [13] G. Giovannetti, P. A. H. Khomyakov, G. Brocks, P. J. Kelly, and J. van den Brink, *Phys. Rev. B* **76**, 073103 (2007).
- [14] S. Lebegue, M. Klintonberg, O. Eriksson, and M. I. Katsnelson, *Phys. Rev. B* **79**, 245117 (2009).
- [15] P. Dutta and P. Horn, *Rev. Mod. Phys.* **53**, 497 (1981).
- [16] Y. K. Pozhela and L. Reggiani, *Hot Electron Transport in Semiconductors* (Springer-Verlag, Berlin, 1985), Chap. 4, p. 113.
- [17] R. F. Voss and J. Clarke, *Phys. Rev. B* **13**, 556 (1976).
- [18] H. Beck and W. Spruit, *J. Appl. Phys.* **49**, 3384 (1978).
- [19] C. J. Stanton and M. Nelkin, *J. Stat. Phys.* **37**, 1 (1984).
- [20] R. Somphonsane, H. Ramamoorthy, G. Bohra, G. He, D. K. Ferry, Y. Ochiai, N. Aoki, and J. P. Bird, *Nano Lett.* **13**, 4305 (2013).
- [21] J. Tworzyl o, B. Trauzettel, M. Titov, A. Rycerz, and C. W. J. Beenakker, *Phys. Rev. Lett.* **96**, 246802 (2006).
- [22] L. DiCarlo, J. R. Williams, Y. Zhang, D. T. McClure, and C. M. Marcus, *Phys. Rev. Lett.* **100**, 156801 (2008).
- [23] R. Danneau, F. Wu, M. F. Craciun, S. Russo, M. Y. Tomi, J. Salmilehto, A. F. Morpurgo, and P. J. Hakonen, *Phys. Rev. Lett.* **100**, 196802 (2008).
- [24] C. J. Stanton and J. W. Wilkins, *Phys. Rev. B* **35**, 9722 (1987).
- [25] K. Van Vliet, J. Fassett, and R. Burgess, *Fluctuation Phenomena in Solids* (Academic Press, New York, 1965), p. 268.
- [26] S. V. Gantsevich, V. L. Gurevich, and R. Katilius, *Riv. Nuovo Cimento* **2**, 1 (1979).
- [27] L. Reggiani, *Hot Electron Transport in Semiconductors* (Springer-Verlag, Berlin, 1985), Chap. 1, p. 7.
- [28] C. Stanton and J. Wilkins, *Physica B&C* **134**, 255 (1985).
- [29] C. J. Stanton and J. W. Wilkins, *Phys. Rev. B* **36**, 1686 (1987).
- [30] F. Green and M. J. Chivers, *Phys. Rev. B* **54**, 5791 (1996).
- [31] F. Green, *Phys. Rev. B* **54**, 4394 (1996).
- [32] F. Green and M. P. Das, *J. Phys.: Condens. Matter* **12**, 5233 (2000).
- [33] F. Green and M. P. Das, *Fluct. Noise Lett.* **1**, C21 (2001).
- [34] V. Bareikis, V. Viktoravichyus, A. Galdikas, and R. Milyushite, *Sov. Phys. Semicond.* **14**, 847 (1980).
- [35] J. Ruch and G. Kino, *Phys. Rev.* **174**, 921 (1968).
- [36] C. E. Korman and I. D. Mayergoyz, *Phys. Rev. B* **54**, 17620 (1996).
- [37] B. Noaman and C. Korman, in *Noise and Fluctuations: 20th International Conference on Noise and Fluctuations*, edited by M. Macucci and G. Basso, AIP Conf. Proc. No. 1129 (AIP, New York, 2009), p. 569.
- [38] M. R. Arai, *Appl. Phys. Lett.* **42**, 906 (1983).
- [39] S. K. Sarker, Y. K. Hu, C. J. Stanton, and J. W. Wilkins, *Phys. Rev. B* **35**, 9229 (1987).
- [40] X. Li, E. A. Barry, J. M. Zavada, M. B. Nardelli, and K. W. Kim, *Appl. Phys. Lett.* **97**, 082101 (2010).
- [41] R. Rengel and M. J. Mart n, *J. Appl. Phys.* **114**, 143702 (2013).
- [42] E. Dutisseuil, A. Sibille, J. Palmier, V. Thierry-Mieg, M. de Murcia, and E. Richard, *J. Appl. Phys.* **80**, 7160 (1996).